Proposal for CLAS Approved Analysis (CAA) for Beam Asymmetry in $\eta' p$, $\pi^0 p$, and $\pi^+ n$ Photoproduction with g8b Data

P. Collins, J. Ball, M. Dugger, E. Pasyuk, B. G. Ritchie
Arizona State University, Tempe, AZ, 85287-1504,
W. J. Briscoe, I. I. Strakovsky, R. L. Workman
The George Washington University, Washington DC, 20052

October 27, 2006

Abstract

We propose to analyze $\eta' p$, $\pi^0 p$, and $\pi^+ n$ photoproduction from the proton using the g8b data taken during summer of 2005. The energy range ($E_\gamma = 1.25 - 2.10 GeV$) of the g8b running period will both complement and extend the world data base for beam asymmetry for $\pi^0 p$ and $\pi^+ n$ photoproduction. For $\eta' p$, any measurements will represent completely new information.

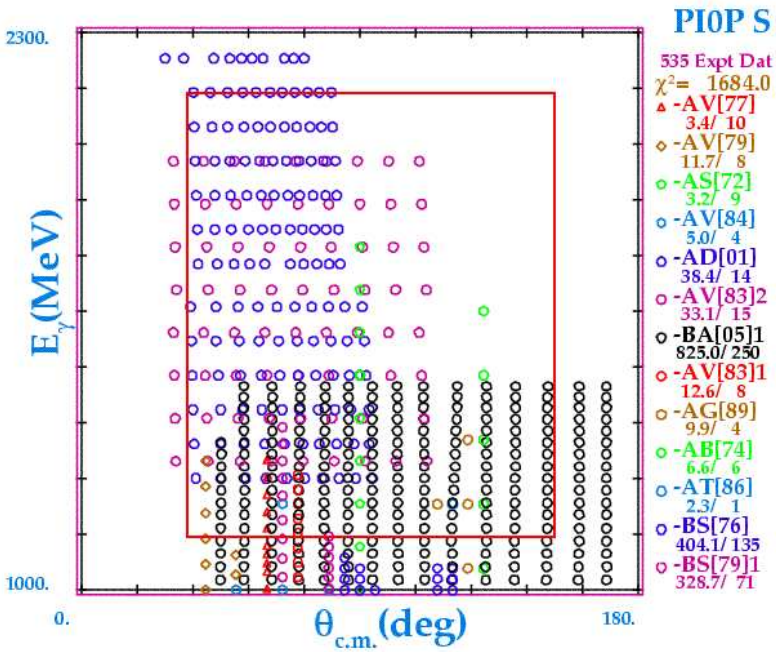

Figure 1: World database for measurements of Σ for $\pi^0 p$ photoproduction. The red box represents the area of expected Σ extraction.

1 Motivation

Much effort is being directed at more fully understanding the internal structure of the proton and neutron. An important tool in this effort is the spectroscopy of their excited states, the nucleon resonances. Results to date [1] have come from a variety of analyses of πN and γN experiments, including traditional Breit-Wigner fits [2, 3] and more sophisticated global, unitary fits [4, 5]. More recently, others have begun to use the measured nucleon resonance properties to probe the internal structure of the states in terms of constituent quark models. Such models explain a significant body of data in terms of quark effective degrees of freedom [6]. Additionally, full quantum chromodynamics calculations of nucleon resonance properties on a lattice are underway [7]. Although these methods describe many types of data, uncertainty about resonance properties and structure remain. An unambiguous understanding of the nucleon resonances demands more extensive measurements.

The challenges presented in understanding nucleon structure are large, in part due to the complexity of this strongly interacting system and to the presence of many broad and overlapping resonances. Of particular interest in investigating nucleon structure, then, are probes that help isolate individual states and ascertain the importance of specific contributions. Since the electromagnetic interaction is so well understood, electromagnetic probes offer one of the more insightful methods for studying the nucleon. The photoproduction reactions $\gamma p \to \eta p$ and $\gamma p \to \eta' p$ are ideal in this regard, since the reaction provides an "isospin filter" to the nucleon response, as ηN and $\eta' N$ final states can only originate (in one-step processes) from isospin I=1/2 systems. Further, as the only isosinglet, η' can be used to indirectly probe gluonic coupling to the proton. (We have already been approved to analyze the reaction $\gamma p \to \eta p$ using g8b data.) The $\pi^0 p$ and $\pi^+ n$ on the other hand will give access to a broad range of N^* and Δ states. These two reactions are fundamental to nuclear interactions, giving us a large $\pi^0 p$ and $\pi^+ n$ signal. The $\pi^0 p$ and $\pi^+ n$ reactions also have

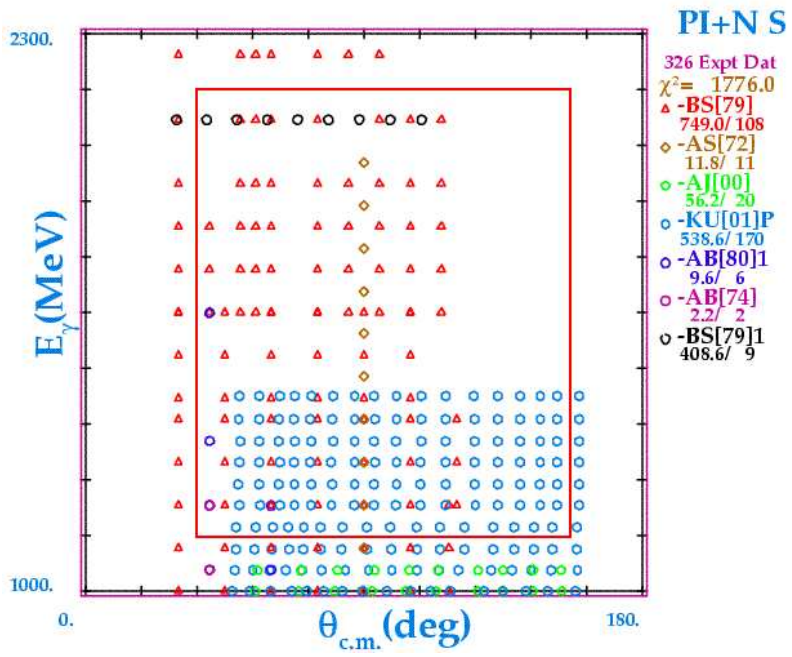

Figure 2: World database for measurements of Σ for $\pi^+ n$ photoproduction. The red box represents the area of expected Σ extraction.

the benefit of a larger signal to background ratio then the $\eta' p$, making the extraction of the $\pi^0 p$ and $\pi^+ n$ peaks easier. We have analyzed ηp, and $\eta' p$ cross sections from the g1 series of experiments in the past [8], [9]. The collaboration recently approved our differential cross sections for $\pi^0 p$ [10], and the ASU group is currently working on $\pi^+ n$ analysis for g1c data.

Figure 1 shows the coverage in photon energy E_γ and scattering angle $\theta_{\text{c.m.}}$ of the available experimental data on the measurement of Σ for $\pi^0 p$ photoproduction, while Fig. 2 shows Σ for the $\pi^+ n$ data.

The data from g8b will allow beam asymmetry measurements to be obtained for $\pi^0 p$ and $\pi^+ n$ in the incident photon energy range of 1.25 to 2.1 GeV. This means that there will be good overlap between world and CLAS data, as well as an extension of the beam asymmetry measurements into uncovered regions.

Using CLAS and the photon tagger, we provided data on the differential cross sections for the reaction $\gamma p \to \eta' p$ [9]. They also show that there is very little information on the photoproduction of $\eta' p$ in the world data. In fact, the majority of the world's data on the photoproduction of $\eta' p$ has come from the previous ASU analysis of CLAS data [9]. The measured differential cross sections are presented in Fig. 3.

The measurements of Σ will be helpful in constraining models of photoproduction. The polarization observables are sensitive to interference between amplitudes allowing better isolation of resonance states. The measurement of these polarization observables will provide constraints to models that cross section measurements alone could not provide. One example of this is seen in Figure 6 [11]. This figure shows comparisons for five different models of η' photoproduction on the proton. The diagrams for the model are included in Figure 7. As stated in [11]

> Diagrams contributing to $\gamma p \to \eta' p$. Time proceeds from right to left. The intermediate baryon states are denoted N for the nucleon and R for the S_{11}, P_{11}, P_{13}, and D_{13} resonances. The intermediate mesons in the t-channel are ρ and ω. The external legs

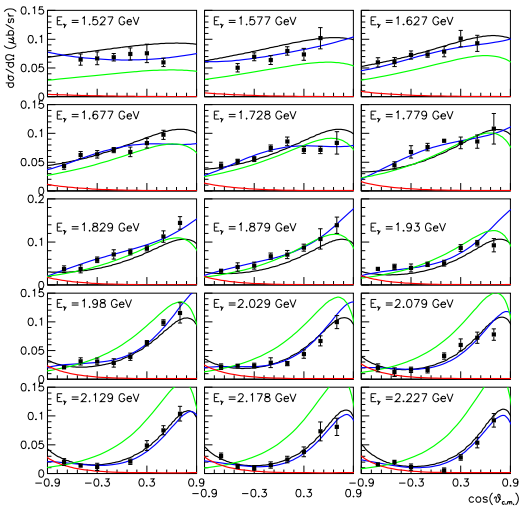

Figure 3: Differential cross sections for η' photoproduction on the proton. Also shown are results from Nakayama and Haberzettl [12] (Red lines: u-channel contributions. Green lines: t-channel contributions. Blue lines: Sum of all s-, t-, and u-channel contributions), and a model (black lines) inspired by A. Sibirtsev *et al.* [13].

> are labeled by the four-momenta of the respective particles and the labels s, u, and t of the hadronic vertices correspond to the off-shell Mandelstam variables of the respective intermediate particles. The three diagrams in the lower part of the diagram are transverse individually; the three diagrams in the upper part are made gauge invariant by an appropriate choice for the contact current depicted in the top-right diagram.

All of the models fit the differential cross sections fairly well, while their predictions for Σ vary greatly. Plots of Σ for $\pi^0 p$ and $\pi^+ n$ showing the SAID and MAID solutions can be found in Figures 4 and 5. From these figures it is easy to see that additional measurements can be of help in refining these models. For these reasons, the measurements of Σ for $\eta' p$, $\pi^0 p$, and $\pi^+ n$ photoproduction should help further our understanding of the nucleon.

Looking at Fig. 8 which shows the missing mass spectrum for the reaction $\gamma p \to pX$ from g1c data for all energy and angle bins, several peaks are clearly identifiable. These peaks are the π^0, η, ρ^0, ω, η', and ϕ. Currently there are analyses planned for the η, ρ^0, ω, and ϕ. Our analysis of the $\pi^0 p$, $\pi^+ n$, and $\eta' p$ would complete this set of analyses, helping maximize the usage of the g8b data set. ASU's experience with the g1 series of experiments makes this analysis of $\pi^0 p$, $\pi^+ n$, and $\eta' p$ a logical follow up to our previous work, and a complement of our current analysis of the beam asymmetry of the η from g8b. GW has expertise in partial-wave analysis, through the SAID program, that will make the analysis of Σ for these reactions a clear extension of their current work.

The analysis of the $\eta' p$ beam asymmetry will provide valuable, previously unknown, data to the world. There are no measurements of $\eta' p$ beam asymmetry, only predictions [11]. Analysis of the $\pi^0 p$ and $\pi^+ n$ beam asymmetry will provide a comparison with current world data and extend it into uncovered regions. This data will not only be very valuable for untangling the N^* states but it will be a clean measurement of beam asymmetry for these reactions. The beam asymmetry will be one of the polarization observables that can be extracted from FROST, but it will be entangled with other observables. This analysis will provide Σ for FROST, which needs Σ to extract beam-target asymmetries, since Σ and these asymmetries are all extracted from ϕ amplitudes, FROST

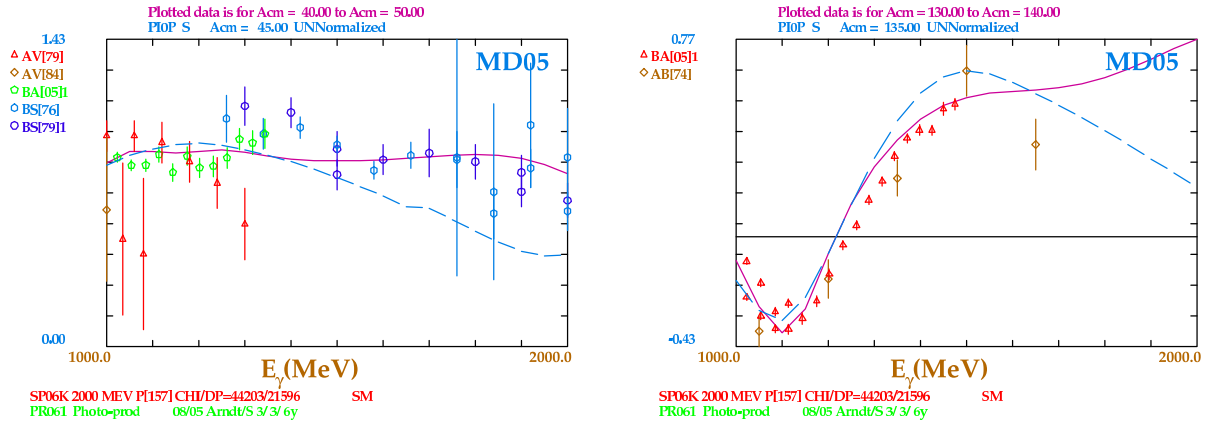

Figure 4: Current existing Σ measurements for $\pi^0 p$ for $\theta_{c.m.} = 45$, and 135 degrees, including SAID (red line) and MAID (blue line) solutions. The left panel shows Σ at $\theta_{c.m.} = 45$ degrees, versus incident photon energy. The right panel shows Σ at $\theta_{c.m.} = 135$ degrees, versus incident photon energy.

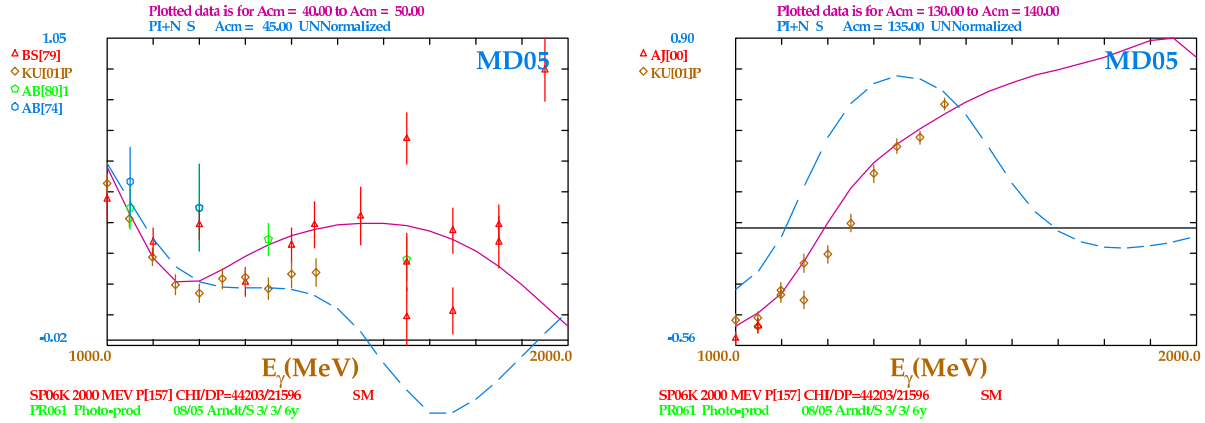

Figure 5: Current existing Σ measurements for $\pi^+ p$ for $\theta_{c.m.} = 45$, and 135 degrees, including SAID (red line) and MAID (blue line) solutions. The left panel shows Σ at $\theta_{c.m.} = 45$ degrees, versus incident photon energy. The right panel shows Σ at $\theta_{c.m.} = 135$ degrees, versus incident photon energy.

will need stand alone measurements of Σ to separate the effects of beam asymmetry from the effects of beam-target asymmetries.

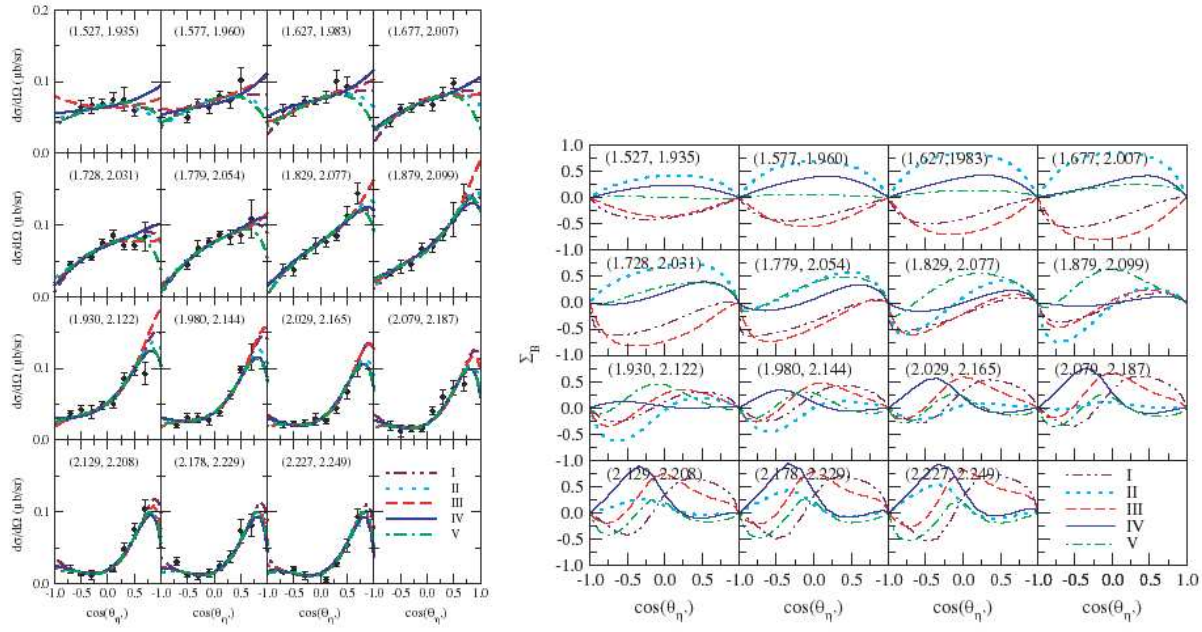

Figure 6: Differential cross sections and beam asymmetry models for $\gamma p \rightarrow \eta' p$ as function of $\cos(\theta^{\eta'}_{c.m.})$, with five models fit to the differential cross sections and the same model predictions for Σ. The numbers (E_γ, W) in parentheses are the incident photon energy E_γ and the corresponding s-channel energy W $=\sqrt{s}$, respectively, in GeV. [11]

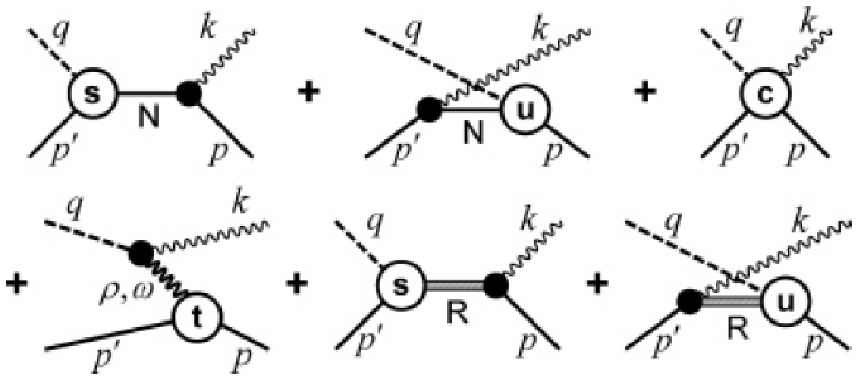

Figure 7: Diagrams for the models of Fig. 6 [11]

2 Yield estimates

Since we have considerable experience in analyzing ηp, $\eta' p$, $\pi^0 p$, and $\pi^+ n$ photoproduction using CLAS data from the g1 series of experiments, we will use this data, when applicable, to estimate the yields to be expected from analyzing g8b.

2.1 Peak identification

The $\pi^0 p$ and $\eta' p$ peaks will be determined through missing mass from the reaction $\gamma p \to pX$ (mass of X is the quantity determined as to be missing). This procedure has been used before by us [8], [9], [10] and was found to be satisfactory in extracting the η, η', and π^0 peak. The left-hand graph in Fig. 8 shows the $\gamma p \to pX$ missing mass spectrum from g1c data for all energy and angle bins. The π^0, η, ρ, ω, and η' peaks are easily identified atop a background dominated by multi-pion events.

The $\pi^+ n$ peak will be determined through missing mass from the reaction $\gamma p \to \pi^+ X$. The right-hand graph in Fig. 8 shows the $\gamma p \to \pi^+ X$ missing mass spectrum from g1c data for all energy and angle bins. The neutron peak is very large and has little background.

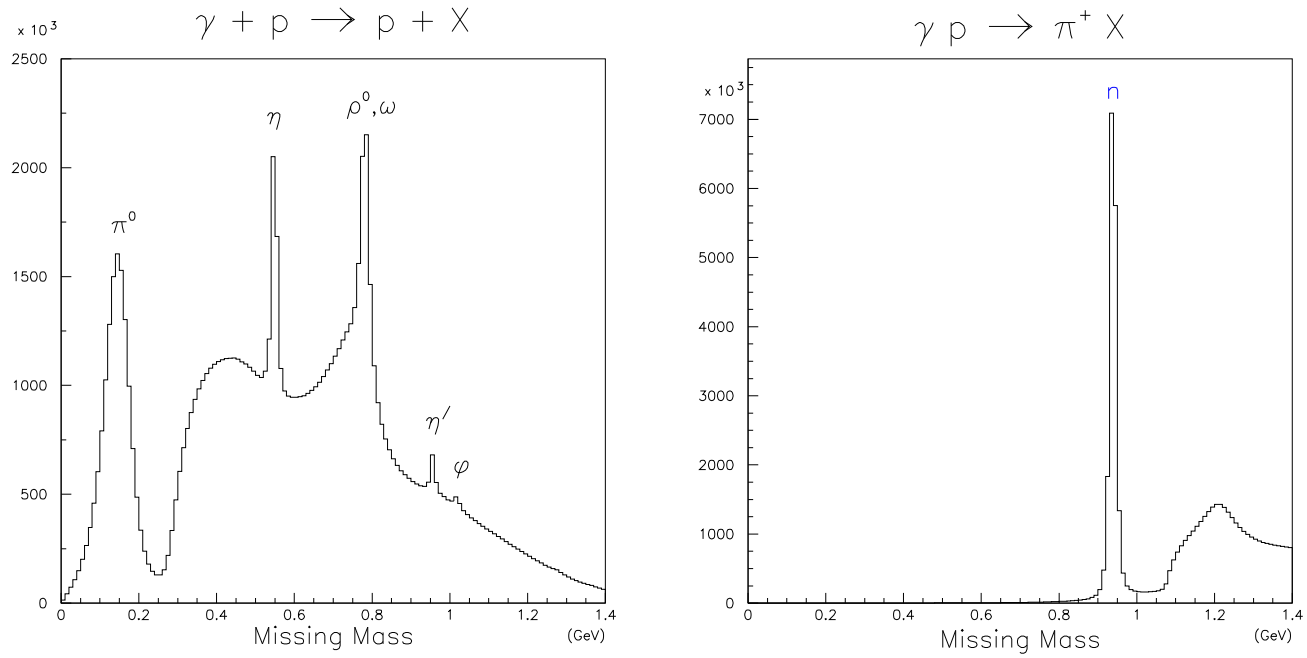

Figure 8: Missing mass spectrum for $\gamma p \to pX$ and for $\gamma p \to \pi^+ X$ from the g1c data set.

2.2 Binning

The full missing mass spectrum described above was broken into bins in photon energy (E_γ) and $\cos(\theta^{\eta'}_{c.m.})$, where $\theta^{\eta'}_{c.m.}$ is the center of mass angle of the η'. The bin sizes chosen were $\Delta E_\gamma = 50$ MeV and $\Delta cos(\theta^{\eta'}_{c.m.}) = 0.2$. The energy and angle binning we will use for the g8b data may be different than that chosen for the g1c data set (this will be determined once we have the actual data in hand). For ease of calculating estimated yields for g8b, the binning scheme for E_γ and $\cos(\theta^{\eta'}_{c.m.})$ described above will be used. For g8b data there will be additional binning in the ϕ direction.

The binning in ϕ will be such that each sector contains two equidistant bins. This means that there will be a bin centered at +8.5 and a bin at -8.5 ° from each sector center of CLAS.

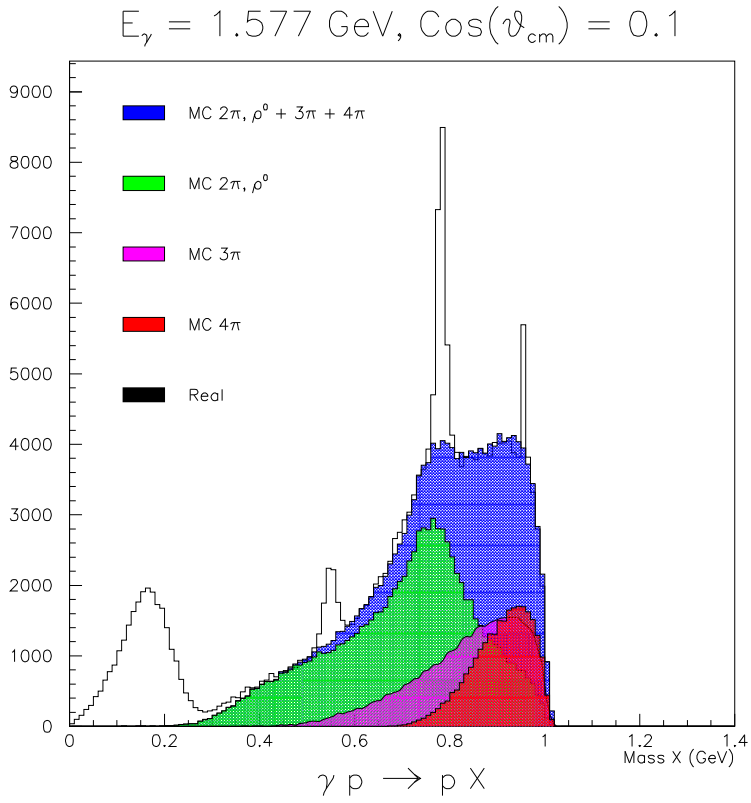

Figure 9: Missing mass spectrum for $\gamma p \to pX$ from the g1c data set.

2.3 Yield estimates

Figure 9 shows a missing mass spectrum of $\gamma p \to pX$ from the g1c data set, for $E_\gamma = 1.577$ GeV and $\cos(\theta^{\eta}_{c.m.}) = 0.1$. The histogram of actual data has superimposed upon it Monte Carlo calculations of the various backgrounds. For purposes of obtaining the best possible background subtraction, the yields of the individual background processes are allowed to vary about the η' peak (0.8 GeV $<$ Missing Mass $<$ 1.1 GeV). To account for possible asymmetries in the background processes, their yields will be fit separately for each bin in $E_\gamma, cos(\theta_{c.m.}), \phi$ space. Once the magnitudes of the individuals backgrounds are determined they are added together and then smoothed and subtracted from the actual data.

The π^0 background was determined by using the shape of the missing mass spectrum from the reaction $\gamma p \to \pi^+\pi^- p$ from the g1 series data. Accidentals were also taken into account. The technique used for accidental determination is covered in our π^0 analysis note[10]. Background for $\gamma p \to \pi^+ n$ was estimated as a 3rd order polynomial.

Once the $\eta' p$, $\pi^0 p$, and $\pi^+ n$ peaks are extracted they are divided by the incident flux (determined by gflux [16]). This result is then divided by the number of bins in ϕ and is defined as $(Y_0)_{ijk}/N_\gamma$ (unpolarized yield per unit flux per bin i,j,k, where i,j,k denotes energy bin, cosine bin, and phi bin).

To obtain the estimated unpolarized yield for each bin, the unpolarized yield per unit flux found from g1c is multiplied by the expected flux for g8b (target length for g1c is identical to that of g8b). Several assumptions were made to estimate the expected flux per bin for g8b:

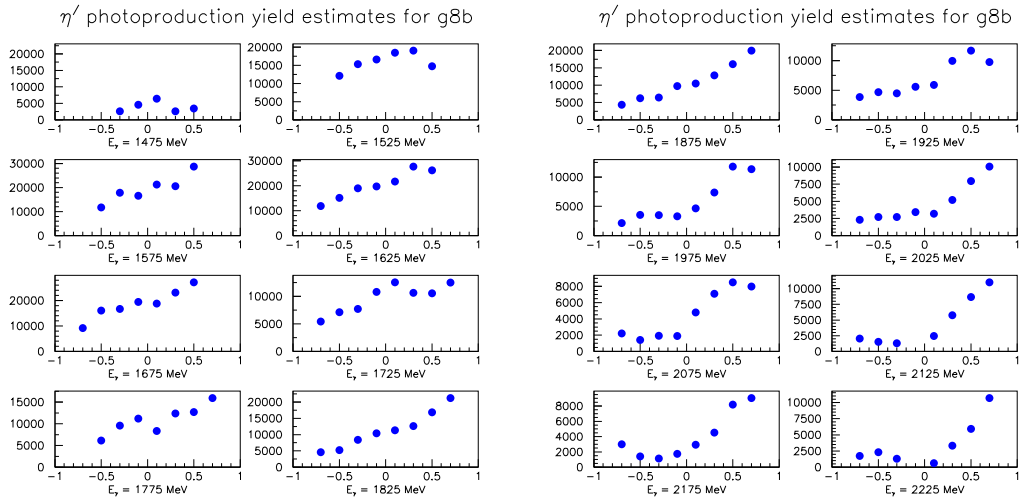

Figure 10: Estimate of η' extraction for E_γ, $\cos(\theta^{\eta'}_{c.m.})$ bins from g8b data.

- the photon flux is constant over the acceptable region
- the acceptable region is from 200 MeV less than the coherent peak to the coherent peak
- the flux over the acceptable region is 5 MHz
- the beam time will be equally split between vertical and horizontal polarization states
- all of the beam time will be used in the analysis (no bad runs).

In addition to the above assumptions, the approximate beam time for each accepted energy region is taken from the records of the g8b run.

Coherent Edge (GeV)	Approx. Beam Time(10^5 Sec)
1.3	3.17
1.5	5.76
1.7	5.02
1.9	2.66
2.1	2.08

Using these assumptions, we can create Fig. 10 which shows our estimated yields of η' for all E_γ and $\cos(\theta^{\eta'}_{c.m.})$ bins of interest to our analysis. From this we can find which E_γ and $\cos(\theta^{\eta'}_{c.m.})$ bins will give an η' yield sufficient for analysis, we are assuming 3000 counts in a cosine bin is sufficient to extract Σ (This would correspond to roughly a 15% statistical error for the yield on each ϕ bin, assuming $\Sigma = 0$). Once these yields are found we can make an estimate of the coverage of our measurements of Σ for $\eta' p$ photoproduction, the expected coverage area is shown in Fig. 11. For $\pi^0 p$ and $\pi^+ n$ the signals are so large that we expect to be able to measure Σ for all coherent edge settings in g8b, and cosine bins from $-0.9 \leq cos(\theta^{\pi}_{c.m.}) \leq 0.9$. Pion binning shall be similar to η'. Estimates of pion yields are available at http://www.jlab.org/Hall-B/secure/g8b/ASU/pi0/ and http://www.jlab.org/Hall-B/secure/g8b/ASU/pipn/.

Estimates for Σ and $\Delta\Sigma$ for the pion reactions are seen in Figures 12 and 12. $\Delta\Sigma$ for the pion reactions is estimated at better then 0.05. The technique used to make these estimates is the same

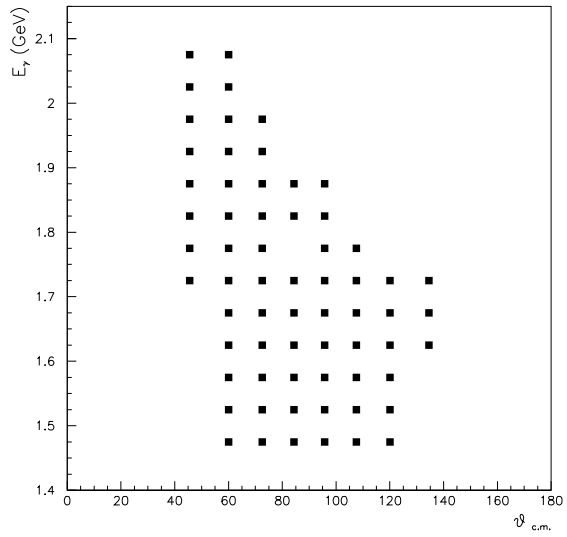

Figure 11: Expected coverage in E_γ and $\theta^{\eta'}_{c.m.}$ of Σ measurement from estimated $\eta' p$ yields.

as that used in our previous CAA [19]. For the η^{prime}, using a Σ of 0.5, estimated uncertainty is 6%

The ASU group has performed a rough preliminary extraction of Σ, for a few $cos(\theta^{\pi}_{c.m.})$ and E_γ bins, for $\pi^0 p$ and $\pi^+ n$. A quick presentation of our technique and result is at http://www.jlab.org/Hall-B/secure/g8b/ASU/quickPiSigma.pdf. Several graphs from this extraction process, and estimates for pion yields, are available at http://www.jlab.org/Hall-B/secure/g8b/ASU/pi0/ and http://www.jlab.org/Ha B/secure/g8b/ASU/pipn/.

3 Conclusion

We have shown that the beam asymmetry for $\eta' p$ photoproduction on the proton should be obtainable using g8b data for the energy range $E_\gamma = 1.5$ to 2.1 GeV. Any measurement of Σ for $\eta' p$ will be in completely unexplored territory. Due to their large signals, measurements of Σ for $\pi^0 p$ and$\pi^+ n$ should be obtainable for all coherent edge settings in g8b, and cosine bins from $-0.9 \leq \cos(\theta^{\pi}_{c.m.}) \leq 0.9$. These measurements will overlap those previously made at other laboratories, many of the measurements will be new to the world. As discussed in the motivation section, these new measurements of Σ can be of use in disentangling the N^* states. In addition to adding to the world database, these measurements will give our group valuable experience in analyzing data using the polarized photon beam that is to be used when the double polarization experiments are underway.

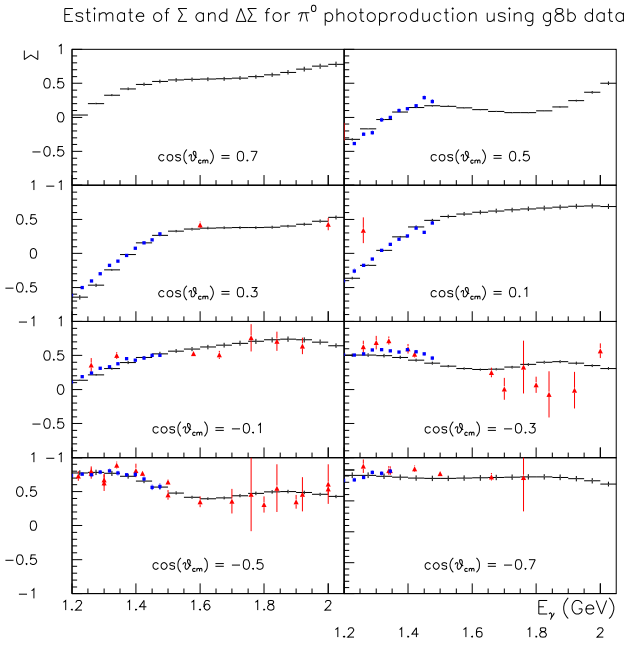

Figure 12: Estimates of Σ and $\Delta\Sigma$ for $\pi^0 p$. Black dots are our estimates, blue dots are GRAAL data and red dots are all data previous to 2000

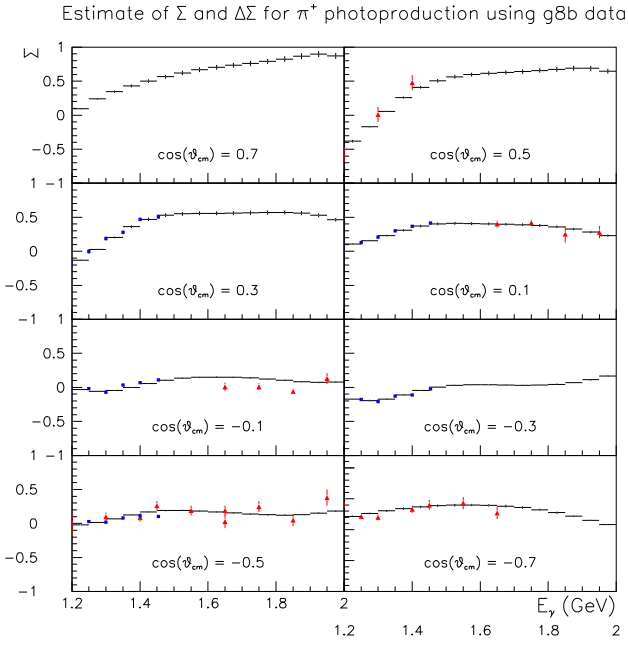

Figure 13: Estimates of Σ and $\Delta\Sigma$ for $\pi^+ n$ Black dots are our estimates, blue dots are GRAAL data and red dots are all data previous to 2000

References

[1] S. Eidelman *et al.*, *The Review of Particle Physics*, Phys. Lett. B**592**, 1 (2004).

[2] For example, H. R. Hicks, S. R. Deans, D. T. Jacobs, P. W. Lyons, and D. L. Montgomery, Phys. Rev. D **7**, 2614 (1973) and D. Drechsel, O. Hanstein, S. Kamalov, and L. Tiator, Nucl. Phys. A **645**, 191 (1999).

[3] W.-T. Chiang, S.-N. Yang, L. Tiator, and D. Drechsel, Nucl. Phys. A **700**, 429 (2002).

[4] R. A. Arndt, I. I. Strakovsky, and R. L. Workman, Phys. Rev. C **62**, 034005 (2000);
R. A. Arndt, I. I. Strakovsky, R. L. Workman, and M. M. Pavan, Phys. Rev. C **52**, 2120 (1995);
R. A. Arndt, I. I. Strakovsky, and R. L. Workman, in: *Proc. of 9th International Symposium on Meson-Nucleon Physics and the Structure of the Nucleon, Washington, DC, USA, July 26–31, 2001*, Eds. H. Haberzettl and W. J. Briscoe, πN Newslett. **16**, 150 (2002).

[5] T. P Vrana, S. A. Dytman, and T.-S. H. Lee, Phys. Reports **328**, 181 (2000).

[6] S. Capstick and W. Roberts, Prog. Part. Nucl. Phys. (Suppl. 2), **45**, S241 (2000).

[7] For example, S. V. Wright, D. B. Leinweber, A. W. Thomas, and K. Tsushima, Nucl. Phys. B Proc. Suppl. **109**, 50 (2002).

[8] M. Dugger, *et al.*, Phys. Rev. Lett. **89**, 222002 (2002).

[9] M. Dugger, *et al.*, Phys. Rev. Lett. **96**, 062001 (2006).

[10] M. Dugger, B.G. Ritchie, J. Ball, P. Collins, and E. Pasyuk, http://www.jlab.org/Hall-B/secure/hadron/analysis_reviews/asu-pizero/pi02006_v3.pdf.

[11] K. Nakayama and H. Haberzettl, Phys. Rev. C **73**, 045211 (2006).

[12] K. Nakayama, and H. Haberzettl, private communication. The results shown here are based on an extended version of the model given in [18].

[13] A. Sibirtsev, Ch. Elster, S. Krewald, and J. Speth, AIP Conf. Proc.**717**, 837 (2004); A. Sibirtsev, Ch. Elster, S. Krewald, and J. Speth, nucl-th/0303044.

[14] JLab Proposal E05-012, "Measurement of Polarization Observables in η-photoproduction with CLAS" Spokespersons: E. Pasyuk (contact), M. Dugger (2005).

[15] JLab Proposal E03-105, "Pion Photoproduction from a Polarized Target", Spokespersons: N. Benmouna, W.J. Briscoe, I.I. Strakovsky, S. Strauch(contact), G.V. O'Rially(2003).

[16] J. Ball, and E. Pasyuk, CLAS note 2005-002.

[17] JLab Update of CLAS g8, "Photoproduction of Vector Mesons and Hyperons with a Beam of Linearly-Polarized Photons", Spokespersons: P.L. Cole (contact), J.C Sanabria, F.J. Klein, J.D. Kellie, K. Livingston, J.A. Nueller, D.J. Tedeschi (2004).

[18] K. Nakayama and H. Haberzettl, Phys. Rev. C **69**, 065212 (2004).

[19] M. Dugger, J. Ball, P. Collins, E. Pasyuk, B. G. Ritchie, "The beam asymmetry in eta photoproduction with g8b data", CLAS Approved Analysis(2006), http://www.jlab.org/Hall-B/secure/hadron/proposals/CAA_eta-photoproduction-g8b.pdf